2021 23rd International Conference on Process Control (PC)
June 1–4, 2021, Štrbské Pleso, Slovakia

Lyapunov Based Adaptive Control for Varying Length Pendulum with Unknown Viscous Friction*

Milan Anderle and Sergej Čelikovský
The Czech Academy of Sciences,
Institute of Information Theory and Automation
(ÚTIA AV ČR),
182 08 Prague 8, Czech Republic
Email: anderle@utia.cas.cz, celikovs@utia.cas.cz

Tomáš Vyhlídal
Department of Instrumentation and Control Engineering,
Faculty of Mechanical Engineering,
and Czech Institute of Informatics, Robotics and Cybernetics,
Czech Technical University in Prague,
Prague 6, Czech Republic,
Email: tomas.vyhlidal@fs.cvut.cz

***Abstract*—Varying length pendulum is studied here to address its oscillations damping using conveniently generated Coriolis force. Lateral damping friction is assumed to be practically negligible and therefore it is not included in the model. Magnitude of the Coriolis force is equal to the product of the angular swing velocity and the velocity of the change of the string length. As a consequence, the problem is modelled by the nonlinear control system having non-controllable and non-stabilizable approximate linearization at the requested damped steady state. Lyapunov technique combined with backstepping design and control Lyapunov function selection is used to tackle this truly nonlinear problem. Furthermore, Lyapunov based adaptive estimation of the viscous friction at the string pivot is designed to improve the controller performance. Besides theoretical mathematical justification the simulations and the real-time experiments using laboratory test-bed are included to highlight the paper results.**

I. Introduction

The topic of the pendulum swing suppression using variation of its string length, as represented by *e.g.* the crane with the suspended load, belongs to the comprehensive area of the flexible systems control intensively studied during five decades [1], [2]. This paper considers the set-up where the string length variation is the only available controlled input as the string pivot is not movable, neither horizontally, nor vertically. At the same time, the lateral friction damping effect is negligible and conveniently generated Coriolis force is the only option to damp the pendulum swing. This feature can be observed in Fig. 4 showing, in particular, the fixed length pendulum swinging (yellow line) during the laboratory experiments showing only a very weak amplitude decrease.

The child swing [3], [4] is the example when Coriolis force is used to pump-up the swing. Here the swing length is fixed, yet Coriolis force is generated by active shifting of the centre of mass of the human sitting on it. Damping pendulum swing motion by controlling the pendulum length only is easier implementable and it has attracted a lot of attention within engineering community [5], [6], [7]. In particular, [8], [9] an open-loop excitation harmonic signal for continuous damping of the pendulum swing was suggested. In contrast, [10] designs the damping signal generated by the feedback using the measurements of the delayed angular position of the pendulum. The Lyapunov based approach to damp the pendulum swing for a pendulum having the controllable rod length has been developed in [11], [12]. Despite some simulation and experimental verification, theoretical justification was rather superficial and did not include the string length convergence. In contrast, the control Lyapunov function (CLF) was successfully used in [13] to design the controller that asymptotically stabilizes the pendulum at the steady downward position with the prescribed nominal string length. Justification included detailed mathematical proof based on rather nontrivial LaSalle principle based analysis of the semi-definiteness of the Lyapunov function derivative along trajectories, as well as simulations and laboratory experiments. Similar Lyapunov based technique was used in [14] to develop the parametrized family of nonlinear passivity-based feedback controllers presenting complementary damping performance for various selections of family members. The backstepping technique is used in [15] to extend the results of [13] to the case where input is considered as the string acceleration, rather then its velocity only.

Viscous friction resisting the pendulum string prolongation and shortening may have significant impact on the string length dynamics. Moreover, its coeffiecient is not precisely known in advance. In such a way, it presents uncertainty in the input channel affecting efficiency of any feedback control strategy, see e.g. the review of friction compensation methods in [16]. Contrary to friction resisting the string control, the lateral friction is negligible, moreover, it may just further help to damp the swing and therefore it may be omitted in the mathematical model of the studied problem.

In this context, the main contribution of this paper is the viscous friction compensation design using yet another modification of the Lyapunov based approach [13], [15]. Note, that the viscous friction is compensated despite the fact that the estimate of the viscous friction coefficient does not converge to its true value. This feature is quite common in adaptive control when system possesses some natural robustness with respect to estimated parameter. As a consequence, the stabilization error converges to zero faster than the estimation error which prevents the latter from vanishing.

The rest of the paper is organized as follows. The next

*Supported by the Czech Science Foundation grant No. 21-03689S.

978-1-6654-0329-0/21/$31.00 ©2021 IEEE

section provides the detailed problem formulation while Section III the controller design presented earlier in [13], [15] is repeated for the reader convenience. The main theoretical result of the paper - the adaptive attenuation of the viscous friction coefficient - is presented in Section IV. Section V collects samples of the simulations and real-time experiments while Section VI concludes the paper.

II. Problem formulation

The setup depicted schematically in Fig. 1 will be studied here. The same set-up was considered in the series of previous articles on the topic of the pendulum swing damping by modifying its length [10], [13], [14], [15]. The pendulum length is adjusted by the movable cart (schematically depicted by the grey rectangle in Fig. 1) applying the force F_u to the cart connected to the suspension string. See also Fig. 3 showing the real experimental test-bed used later on to verify the performance of designed controllers.

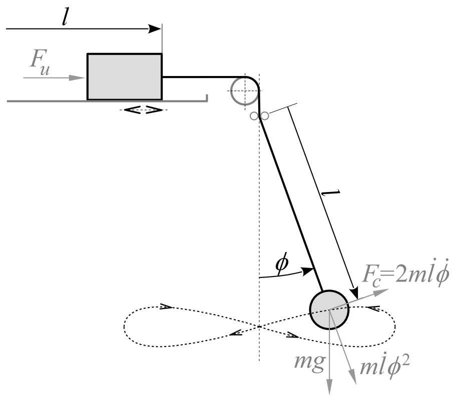

Fig. 1. The cart-pendulum setup to damp the swing using the Coriolis force.

In order to model this set-up, the idealized pendulum with the adjustable string length is considered. Neglecting the mass of the string and the lateral friction resisting the pendulum swinging, the governing equation of motion is given by the following nonlinear second order system

$$ml(t)\ddot{\phi}(t) + 2m\dot{l}(t)\dot{\phi}(t) + mg\sin\phi(t) = 0, \tag{1}$$

where $\phi(t), l(t)$ denote the pendulum angle and length of the string, respectively, m is the mass of the load and g is the gravitational acceleration. Here, the term $2m\dot{l}(t)\dot{\phi}(t)$ actually represents the mentioned Coriolis force. The equation (1) is coupled with the equation describing the dynamics of the string length, namely:

$$m\ddot{l}(t) = ml(t)\dot{\phi}^2(t) + mg\cos\phi(t) - F(t) + k_{visc}\dot{\phi}(t), \tag{2}$$

where $F(t) := -F_u$ shown in Fig. 1. First term on the right-hand side of (2) represents the centrifugal force, next to it the gravitation, while the last one attenuates the viscous friction of both the cart and string at the pivot mechanism. Its coefficient $k_{visc} > 0$ is known only approximately. All variables, parameters and forces are depicted in Fig. 1 as well.

As explained in Section V in detail, the variables ϕ and l are measured by convenient sensors. The pendulum damping problem can be therefore viewed as the asymptotic feedback stabilization of some equilibrium of the properly defined state space representation of (1)-(2).

The control design in [13], [14] used the three-dimensional state space representation of (1) considering $\dot{l}$ as the controlled input and ignoring (2), namely

$$\begin{aligned} \dot{x}_1 &= x_2, \\ \dot{x}_2 &= -\frac{1}{x_3}(2x_2u + g\sin x_1), \\ \dot{x}_3 &= u, \end{aligned} \tag{3}$$

$$x_1 = \phi(t),\ x_2 = \dot{\phi}(t),\ x_3 = l(t),\ u(t) = \dot{l}(t). \tag{4}$$

Practical considerations require that

$$x_1 \in [-\pi/2, \pi/2], \quad x_2 \in \mathbb{R}, \quad x_3 > 0. \tag{5}$$

Indeed, recall that x_3 is the string length and x_1 is the angle of the string with respect to a vertical line, so that $|x_1| > \pi/2$ would cause, at least initially, the free fall of the mass rather than the pendulum like movement.

Further, denote $x = (x_1, x_2, x_3)^\top$. The desired nominal equilibrium of (3) to be stabilized is $x^{eq} = (0, 0, l_0)^\top$, where l_0 is some desired nominal length of the string. The approximate linearization of (3) around its equilibrium $x^{eq} = (0, 0, l_0)^\top$ is given by the following pair

$$\begin{bmatrix} 0 & 1 & 0 \\ -g/l_0 & 0 & 0 \\ 0 & 0 & 0 \end{bmatrix}, \quad \begin{bmatrix} 0 \\ 0 \\ 1 \end{bmatrix}, \tag{6}$$

which is neither controllable nor stabilizable. Indeed, it possesses the pair of complex conjugated uncontrollable eigenvalues. Therefore, the full nonlinear model has to be taken into the account to be asymptotically stabilized by the smooth state feedback. Moreover, exponential stabilization of (3) by a smooth feedback is excluded [17]. In this vein, [13] used CLF approach and designed the feedback controller

$$u(x) = -K\left(g(1 - \cos x_1) - x_3x_2^2 + c_1(x_3 - l_0)\right), \tag{7}$$

which asymptotically stabilizes the system (3) from a large region of attraction for any design parameters $K > 0$, $c_1 > 0$.

As the real input is the force F acting on the cart, the experimental laboratory implementation of the controller (7) required in [13] additional proportional derivative (PD) cascade. More specifically, based on the real-time measurements of $l, \dot{l}, \phi, \dot{\phi}$ and realizing that $x = (\phi, \dot{\phi}, l)^\top$ the error signal $e = u(x) - \dot{l}$ was generated and numerically differentiated to get $\dot{e}$. Then, the cart was controlled by $F = Pe + D\dot{e}$ and damping performance was improved by laborious manual "intuitive" tuning of P, D coefficients. The same approach was applied in [14] to implement alternative passivity-based controllers.

As a moderate improvement, the equation (2) could be used to compensate all its terms precisely, except the unknown viscous friction. Namely, implement the force

$$F(t) = ml(t)\dot{\phi}^2(t) + mg\cos\phi(t) - m\left(Pe + D\dot{e}\right).$$

By (2) the last equality is equivalent to $\ddot{l} = Pe + D\dot{e} - k_{visc}\dot{\phi}$ which provides better chances for successful P,D tuning.

Visible drawbacks of these implementations are both theoretical (there is not rigorous justification of the overall convergence of the scheme involving the additional PD cascade) and practical (necessity of a lengthy manual controller tuning for any change of parameters).

To remove these drawbacks, the following four-dimensional state space model was considered in [15]:

$$\begin{array}{rcl} \dot{x}_1 &=& x_2 \\ \dot{x}_2 &=& -\frac{1}{x_3}(2x_2x_4 + g\sin x_1) \\ \dot{x}_3 &=& x_4 \\ \dot{x}_4 &=& \overline{u} - m^{-1}k_{visc}x_4, \end{array} \tag{8}$$

$$x_1 := \phi(t),\ x_2 := \dot{\phi},\ x_3 := l,\ x_4 := \dot{l}, \tag{9}$$

$$\overline{u} = \ddot{l} = l\dot{\phi}^2 + g\cos\phi - F/m. \tag{10}$$

The "virtual" input (10) is easily implementable by feedback transformation from the controlled (in reality) force F to the virtual input $\overline{u} := \ddot{l}$ in (2). Indeed, knowing any state feedback controller for $\overline{u}$ one can easily implement a corresponding controller for F inverting (10):

$$F(t) = ml(t)\dot{\phi}^2(t) + mg\cos\phi(t) - m\overline{u}. \tag{11}$$

Throughout the rest of the paper denote $x = (x_1, x_2, x_3, x_4)^\top$. Again, it is easy to check that the approximate linearization of (8) at the equilibrium $(0,0,l_0,0)^\top$ to be stabilized is neither controllable, nor stabilizable.

III. Backstepping design

Let throughout this section $k_{visc} = 0$. The state space model (8) is the result of "adding (an) integrator" to (3). The backstepping methodology [17] provides the tool how to construct the asymptotically stabilizing controller for (8) based on the knowledge of (7) and the respective Lyapunov function, in particular, showing in [15] that $\forall c_1 > 0$, $K > 0$, $K_2 > 0$

$$\begin{array}{l} \overline{u}(x) = -K\left(gx_2\sin x_1 - x_4x_2^2 + 2x_2(2x_2x_4 + g\sin x_1) + c_1x_4\right) \\ \quad -(K_2K+1)\left(g(1-\cos x_1) - x_3x_2^2 + c_1(x_3 - l_0)\right) - K_2x_4, \end{array} \tag{12}$$

asymptotically stabilizes (8) at $(0,0,l_0,0)^\top$.

Let us repeat here the backstepping procedure from [15] deriving the controller (12) stabilizing asymptotically (8).

First, construct the control Lyapunov function (CLF):

$$\overline{V} = gx_3(1-\cos x_1) + \frac{x_3^2x_2^2}{2} + c_1\frac{(x_3 - l_0)^2}{2} \tag{13}$$

$$+ \frac{\left(x_4 + K\left(g(1-\cos x_1) - x_3x_2^2 + c_1(x_3 - l_0)\right)\right)^2}{2}. \tag{14}$$

Actually, (13) represents Lyapunov function proving the asymptotic stability of (3), (7) while the term in (14) penalizes the difference between x_4 and (7).

Secondly, compute the full time derivative of $\overline{V}$ along the trajectories of (8) denoted as $\dot{\overline{V}}$ depending on $\overline{u}$ and design $\overline{u}$ making $\dot{\overline{V}}$ negative definite, or at least semi-definite. In this way, CLF $\overline{V}$ becomes Lyapunov function proving stability. More specifically, recalling the assumption $k_{visc} = 0$ it holds

$$\begin{array}{l} \dot{\overline{V}} = \left(g(1-\cos x_1) - x_3x_2^2 + c_1(x_3 - l_0)\right)x_4 + \\ \left(x_4 + K\left(g(1-\cos x_1) - x_3x_2^2 + c_1(x_3 - l_0)\right)\right)\left(\overline{u} + \right. \\ \left. K\left(gx_2\sin x_1 - x_4x_2^2 + 2x_2(2x_2x_4 + g\sin x_1) + c_1x_4\right)\right). \end{array} \tag{15}$$

Substituting $\overline{u}$ from (12) and using the notation (7) gives

$$\dot{\overline{V}} = -K^{-1}u(x)^2 - K_2(x_4 - u(x))^2 \le 0,\ K > 0, K_2 > 0. \tag{16}$$

Since $\dot{\overline{V}}$ is negative semi-definite, Lyapunov stability of (8), (12) has been proved. Asymptotic stability can be proved either making $\dot{\overline{V}}$ negative definite, or using LaSalle invariance principle (LSIP). Since the former seems to be impossible, the latter option is to be used. To recall LSIP, denote

$$\overline{V}_{d,0} = \{x \in \mathbb{R}^4 \,|\, \dot{\overline{V}}(x) = 0\}.$$

By LSIP the equilibrium $(0,0,l_0,0)^\top$ of (8), (12) is asymptotically stable if the largest invariant subset of $\overline{V}_{d,0}$ with respect to (8), (12) contains the point $(0,0,l_0,0)^\top$ only. Realize that $x \in \overline{V}_{d,0}$ if and only if $u(x) = 0 \wedge x_4 = 0$ giving by (7)

$$g(1-\cos x_1) - x_3x_2^2 + c_1(x_3 - l_0) = 0, \quad x_4 = 0.$$

Invariance with respect to trajectories of (8) implies that full time derivatives of the above equalities along trajectories of (8) hold as well. This gives

$$gx_2\sin x_1 - x_4x_2^2 + 2x_2x_3\frac{1}{x_3}(2x_2x_4 + g\sin x_1) + c_1x_4 = 0.$$

By $x_4 = 0$ the last equality gives $x_2\sin x_1 = 0$. Differentiating $x_2(t)\sin x_1(t) = 0$ with respect to time along trajectories of (8)

$$-x_3^{-1}g\sin^2 x_1 + x_2^2\cos x_1 = 0, \quad \text{again, since } x_4 = 0.$$

Summarizing, we have shown that any solution $x(t)$ of (8), such that $x(t) \in \overline{V}_{d,0}$, $\forall t \ge 0$, it holds that

$$x_4 = 0,\ g(1-\cos x_1) - x_3x_2^2 + c_1(x_3 - l_0) = 0, \tag{17}$$

$$x_2\sin x_1 = 0,\ \ x_3^{-1}g\sin^2 x_1 - x_2^2\cos x_1 = 0. \tag{18}$$

Since $x_1 \in (-\pi/2, \pi/2)$ and $x_3 > 0$, the two equalities in (18) imply together that $x_1 = x_2 = 0$. Indeed, by the first equality in (18) either $x_2 = 0$ or $\sin x_1 = 0$, *i.e.* $x_1 = 0$ by $x_1 \in (-\pi/2, \pi/2)$. Now, substituting $x_1 = 0$ into the second equality in (18) gives by $\cos x_1 \ne 0$ that $x_2 = 0$ while substituting $x_2 = 0$ into the second equality in (18) gives $x_1 = 0$.

Next, substituting $x_1 = x_2 = 0$ to the second equality in (17) gives for $c_1 > 0$ that $x_3 = l_0$. In such a way, the set $\{x \in \mathbb{R}^4 \,|\, x = (0,0,l_0,0)^\top\}$ is the only subset of the set $\overline{V}_{d,0}$ that is invariant with respect to trajectories of (8), (12). By LISP the equilibrium $(0,0,l_0,0)^\top$ is asymptotically stable and the following result has been proved.

Proposition 3.1: [15] Let $K > 0, K_2 > 0, c_1 > 0$ are given. Consider the system (8) in the region $\mathscr{D} \times \mathbb{R}$, $\mathscr{D} = (-\pi/2, \pi/2) \times \mathbb{R} \times (0, \infty)$. Then the feedback (12) asymptotically stabilizes the system (8) at the equilibrium $(0,0,l_0,0)^\top$ and its region of attraction is the largest subset of $\mathscr{D} \times \mathbb{R}$ which is invariant with respect to trajectories of (8) and (12).

IV. MAIN RESULT - VISCOUS FRICTION ATTENUATION

In the sequel, the vicsous friction coefficient $k_{visc} > 0$ in (8) is assumed to be nonzero and unknown. Denote by $\overline{k}_{visc} := m^{-1}k_{visc}$ the "mass-normalized" viscous friction coefficient, then the fourth equation in (8) becomes $\dot{x}_4 = \overline{u} - \overline{k}_{visc}x_4$. The adaptive controller to attenuate an unknown $\overline{k}_{visc} > 0$ is constructed as follows

$$\begin{aligned}\overline{u} = \overline{u}_{ad}(x,x_5) = -K\times \\ \left(gx_2\sin x_1 - x_4x_2^2 + 2x_2(2x_2x_4 + g\sin x_1) + c_1x_4\right) \\ -(K_2K+1)\left(g(1-\cos x_1) - x_3x_2^2 + c_1(x_3 - l_0)\right) \\ -K_2x_4 + x_5x_4, \quad \dot{x}_5 = -\sigma x_4(x_4 - u(x)),\end{aligned} \tag{19}$$

where $c_1 > 0,\ K > 0,\ K_2 > 0, \sigma > 0$ are arbitrarily selected design parameters, $u(x)$ is defined in (7). As a matter of fact, x_5 serves as the estimate of the "mass-normalized" viscous friction coefficient $\overline{k}_{visc}$, while the dynamic equation for x_5 is the adaptation law.

The system (8) with $\overline{u} = \overline{u}_{ad}(x)$ given by (19) becomes

$$\begin{aligned}\dot{x}_1 &= x_2 \\ \dot{x}_2 &= -\tfrac{1}{x_3}(2x_2x_4 + g\sin x_1) \\ \dot{x}_3 &= x_4 \\ \dot{x}_4 &= \overline{u}_{ad}(x,x_5) - \overline{k}_{visc}x_4 \\ \dot{x}_5 &= -\sigma x_4(x_4 - u(x))\end{aligned} \tag{20}$$

$$x_1 := \phi(t),\ x_2 := \dot{\phi},\ x_3 := l,\ x_4 := \dot{l},\quad x_5 \in \mathbb{R}. \tag{21}$$

Formally, (20) is the five-dimensional state space system, though the state variable x_5 actually represents the estimate of an unknown $\overline{k}_{visc}$. Moreover, the task is to stabilize asymptotically x_1, x_2, x_3, x_4 to the equilibrium $(0,0,l_0,0)^\top$, while the precise asymptotic behavior of x_5 is not required.

To study the above task, consider Lyapunov-like function

$$V_{ad}(x,x_5) = \overline{V} + (x_5 - \overline{k}_{visc})^2/(2\sigma), \tag{22}$$

where $\overline{V}$ is given by (13), (14). An unknown $\overline{k}_{visc} > 0$ is a constant, therefore the last equation of (20) gives

$$\dot{V}_{ad} = \dot{\overline{V}} - (x_5 - \overline{k}_{visc})x_4(x_4 - u(x)). \tag{23}$$

Here, $\dot{\overline{V}}$ stands for the full time derivative of $\overline{V}$ given by (13), (14) with respect to trajectories of (20) and therefore

$$\begin{aligned}\dot{\overline{V}} = \left(g(1-\cos x_1) - x_3x_2^2 + c_1(x_3 - l_0)\right)x_4 + \\ (x_4 - u(x))) \times \\ \left(\overline{u}_{ad}(x,x_5) + K\left(gx_2\sin x_1 - x_4x_2^2 + 2x_2(2x_2x_4 + g\sin x_1) + c_1x_4\right)\right) \\ +(x_4 - u(x))(-\overline{k}_{visc}x_4).\end{aligned}$$

Recall that $u(x)$ is given by (7) and therefore by (19) and (23)

$$\begin{aligned}\dot{V}_{ad} = -K^{-1}u(x)x_4 \\ +(x_4 - u(x))\left((K_2K+1)u(x)K^{-1} - K_2x_4 + x_5x_4\right) \\ +(x_4 - u(x))(-\overline{k}_{visc}x_4) \\ -x_4x_5(x_4 - u(x)) + \overline{k}_{visc}x_4(x_4 - u(x)).\end{aligned}$$

Further simple manipulations and terms cancelations give

$$\dot{V}_{ad} = -K^{-1}(u(x))^2 - K_2(x_4 - u(x))^2 \le 0. \tag{24}$$

By (24) the equilibrium $(0,0,l_0,0,\overline{k}_{visc})^\top$ is Lyapunov stable with respect to (20). Note that the mentioned equilibrium is not completely known, as its last component is the unknown parameter $\overline{k}_{visc}$.

To prove asymptotic stability, LaSalle principle based analysis mimicking almost exactly the one following after (16) is needed. Indeed, again the set where $\dot{V}_{ad} = 0$ is given by $u(x) = 0 \wedge x_4 = 0$. Realize that for $x_4 = 0$ the first four equations of (20) became the same as (8). Further, $u(x)$ depends on x_1, x_2, x_3 only and therefore the analysis performed between (16) and Proposition 3.1 can be exactly repeated to conclude that any point from largest invariant subset of the set where $\dot{V}_{ad} = 0$ satisfies $x_1 = x_2 = x_3 - l_0 = x_4 = 0$.

Nevertheless, now comes the difference caused by the adaptive extension by coordinate x_5 added to estimate $\overline{k}_{visc}$. No specific condition for x_5 can be derived in this specific case. As a consequence the largest invariant set inside the set where $\dot{V}_{ad} = 0$ contains the nontrivial set

$$\{x \in \mathbb{R}^5 \,|\, x_1 = x_2 = x_3 - l_0 = x_4 = 0, x_5 \in \mathbb{R}\}.$$

Indeed, to double check that the above set is indeed invariant, substitute $x_1 = x_2 = x_3 - l_0 = x_4 = 0,\ x_5 = x_5^0 \in \mathbb{R}$ to (20) gives $\dot{x}_1 = \dot{x}_2 = \dot{x}_3 = \dot{x}_4 = \dot{x}_5 = 0$. In such a way, for any chosen $x_5^0 \in \mathbb{R}$ the set

$$\{x \in \mathbb{R}^5 \,|\, x_1 = x_2 = x_3 - l_0 = x_4 = 0, x_5 = x_5^0 \in \mathbb{R}\}$$

is invariant with respect to trajectories of (20). Actually, it is a single point being the equilibrium of (20). Finally, recall that any union of invariant sets is itself invariant. This gives the following result.

Proposition 4.1: Recall (22). Let $R > 0$ be such that

$$V_{ad}(x,x_5) < R \quad \Rightarrow \quad x_1 \in (-\pi/2, \pi/2) \wedge x_3 > 0.$$

Then for any $x(0), x_5(0)$ such that $V_{ad}(x(0), x_5(0)) < R$ the solution $x(t), x_5(t)$ of the system (20) satisfies that

$$\lim_{t\to\infty} x(t) = (0,0,l_0,0)^\top$$

and $x_5(t)$ is bounded for $t \in [0,\infty)$.

Proof: Convergence of $x(t)$ was proved during the exposition before. The set of initial conditions is easily verified since the function $V_{ad}(x,x_5)$ is non-increasing along trajectories. Moreover, since $R > V_{ad}(x(t), x_5(t)) \ge (x_5(t) - \overline{k}_{visc})^2/(2\sigma)$, the function $x_5(t)$ is bounded. ■

Remark 4.2: The right hand side in (24) exactly coincides with that of (16). In other words, the full time derivative of V_{ad} (containing unknown parameter) along trajectories of (20) (containing unknown parameter) is exactly the same as that of $\overline{V}$ along trajectories of (8) **without** unknown parameter. This constitutes actually the very essence of **Lyapunov based adaptive design**. The fact that $x_5(t)$, in general, need not converge to $\overline{k}_{visc}$ is caused by the specific form of the unknown term $\overline{k}_{visc}x_4$, so it vanishes for $x_4 = 0$. This situation is usually called as **adaptive controller without identification**.

V. SIMULATIONS AND EXPERIMENTS

The aim of this section is to compare performance of the controller (12) ignoring the viscous friction with the controller (19) that adaptivelly attenuates it. Both simulation numerical experiments and real-time experiments were carried out.

First, Fig. 2 shows the simulation comparision. The nominal string length is taken as $l_0 = 1$m and initial conditions as $l(0) = l_0$, $\dot{l}(0) = 0$ and $\phi(0) = \pi/2$, $\dot{\phi}(0) = 0$. The simulation model included some viscous friction but its value was not used in controllers. While in (12) it was ignored completely, its adaptive estimation was used in (19).

Top sub-figure of Fig. 2 compares the angle ϕ courses both for (12) (blue) and (19) (red). For the reference, the fixed length pendulum oscillations are also included.

The respective string length l courses are shown by the middle sub-figure of Fig. 2, again the blue line corresponds to (12) while the red one to (19).

The bottom sub-figure of Fig. 2 shows the evolution of the viscous friction coefficient estimate evolution. As predicted theoretically, it converges to a value that differs from "unknown" value used in simulation model shown by dotted line. The difference between damping performances of adaptive and

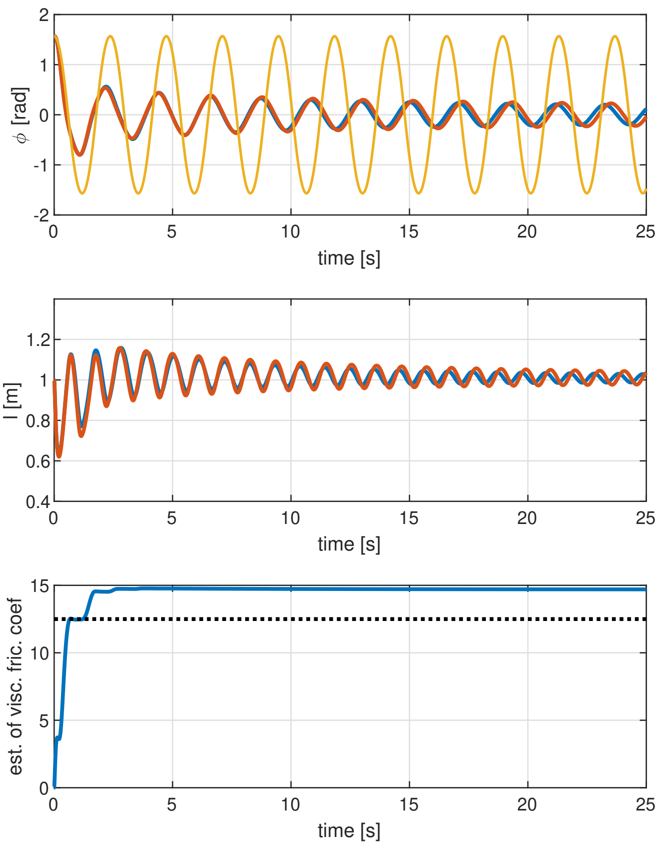

Fig. 2. Simulation of controllers performance with and without adaptation.

non-adaptive controllers is minor only. This has a common reason with mentioned lack of parameter estimate to its true value. Indeed, non-adaptive controller itself is robust with respect to friction effect, therefore it does not generate a "sufficiently rich" error signal to speed up the estimate convergence.

Secondly, controllers were compared in laboratory real-time experiments. The platform depicted in Fig. 3 was used. It consists of rails with a movable cart controlled by a DC motor via the belt and the fixed base consisting of pulley with the arm equipped by the rotational sensor to measure the pendulum angle. The pendulum string (highlighted in red) is connected to the movable cart and passes through the pulley with the arm. The pendulum string length is controlled applying force to the movable cart by the DC motor. The viscous friction to be compensated occurs partly between the rails and the movable cart as well as between string and the pulley with arm. The DC motor is commanded from cRIO controller via an industrial control unit.

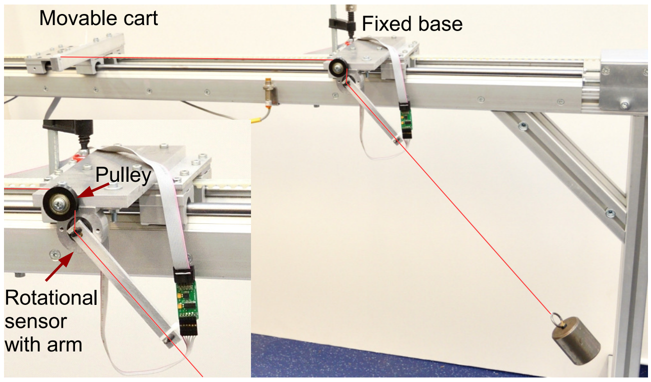

Fig. 3. The experimental test-bed for the varying pendulum swing.

In all experiments the nominal string length is $l_0 = 0.6$ m, initial conditions are $l(0) = l_0$, $\dot{l}(0) = 0$, $\dot{\phi}(0) = 0$, while $\phi(0)$ is set by manual lifting the load and is not known precisely.

Fig 4 shows the experimental course of the angle ϕ both for uncompensated friction controller (12) (blue) and the compensated friction controller (19) (red). Yellow line shows freely swinging fixed length pendulum subject only to a very weak natural damping by air resistance of pulley with arm sensor influence. The corresponding string length course is shown in Fig. 5, the colors correspond to those for angle ϕ courses.

Finally, the viscous friction coefficient estimation is shown in Fig. 6. The top section shows the course of the estimation of the viscous friction parameter during one experiment. The bottom section then collects further repeated experiments. Blue lines stand for coefficient estimate while the red ones for pendulum swing angle.

All repeated experiments in Fig. 6 gave very similar results of the coefficient estimate. As a consequence, one may heuristically conclude that these values might be close to the real unknown coefficient value. Note also that the damping in experiment shown in Fig 4 is visibly better for adaptive control than for the controller ignoring the friction.

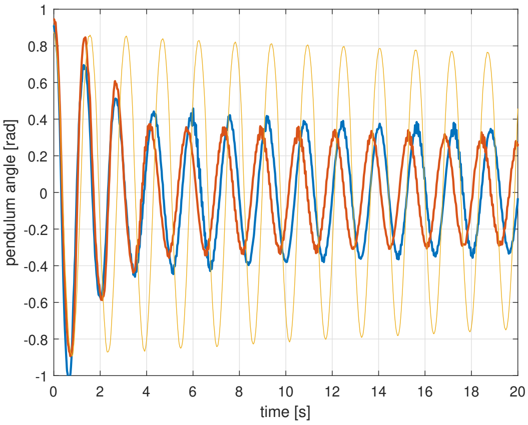

Fig. 4. Experimental comparision of controllers with and without adaptation.

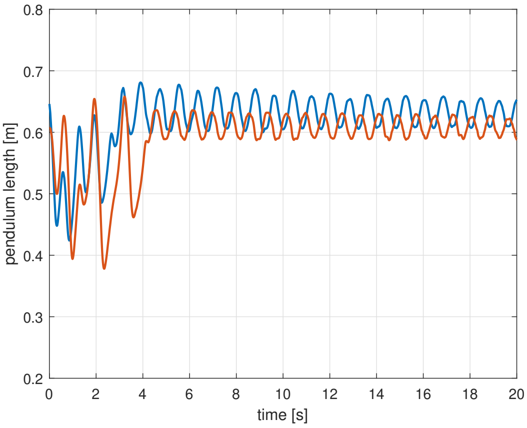

Fig. 5. The time evolution of the pendulum length in experiments.

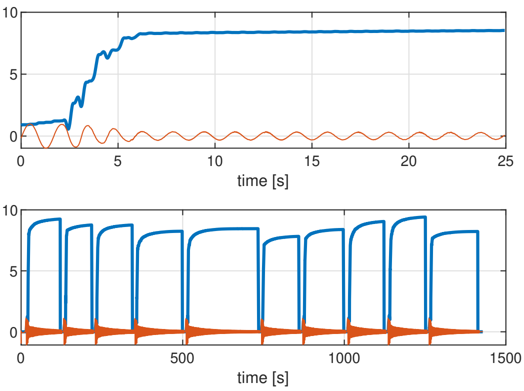

Fig. 6. Experiments: top - estimation detail of the viscous friction parameter; bottom - repeated estimation of the viscous friction parameter.

VI. Conclusions and Outlook

Theoretical development of the viscous friction adaptive compensation was proposed and fully theoretically justified. While simulations did not show a visible difference between adaptive and non-adaptive controllers, experimental results were slightly, yet visibly, in favor of the adaptive controllers.

The outlook for future research is to use the developed adaptive viscous friction compensation for tracking the non-vanishing reference where its prevalence compared to non-adaptive control scheme should be more visible. Indeed, in case of damping the friction decays with decaying string velocity and its coefficient may not have so heavy influence.

References

[1] W. Singhose, "Command shaping for flexible systems: A review of the first 50 years," *International Journal of Precision Engineering and Manufacturing*, vol. 10, no. 4, pp. 153–168, 2009.

[2] L. Ramli, Z. Mohamed, A. M. Abdullahi, H. Jaafar, and I. M. Lazim, "Control strategies for crane systems: A comprehensive review," *Mechanical Systems and Signal Processing*, vol. 95, pp. 1 – 23, 2017.

[3] B. Piccoli and J. Kulkarni, "Pumping a swing by standing and squatting: do children pump time optimally?" *IEEE Control Systems*, vol. 25, no. 4, pp. 48–56, 2005.

[4] S. Wirkus, R. Rand, and A. Ruina, "How to pump a swing," *The College Mathematics Journal*, vol. 29, no. 4, p. 266, 1998.

[5] A. Pinsky and A. Zevin, "Oscillations of a pendulum with a periodically varying length and a model of swing," *International Journal of Non-Linear Mechanics*, vol. 34, no. 1, pp. 105 – 109, 1999.

[6] A. Belyakov, A. Seyranian, and A. Luongo, "Dynamics of the pendulum with periodically varying length," *Physica D: Nonlinear Phenomena*, vol. 238, no. 16, pp. 1589 – 1597, 2009.

[7] F. Reguera, F. E. Dotti, and S. P. Machado, "Rotation control of a parametrically excited pendulum by adjusting its length," *Mechanics Research Communications*, vol. 72, pp. 74–80, 2016.

[8] D. Stilling and W. Szyszkowski, "Controlling angular oscillations through mass reconfiguration: a variable length pendulum case," *International Journal of Non-Linear Mechanics*, vol. 37, no. 1, pp. 89 – 99, 2002.

[9] W. Szyszkowski and D. Stilling, "On damping properties of a frictionless physical pendulum with a moving mass," *International Journal of Non-Linear Mechanics*, vol. 40, no. 5, pp. 669 – 681, 2005.

[10] T. Vyhlídal, M. Anderle, J. Bušek, and S. Niculescu, "Time-delay algorithms for damping oscillations of suspended payload by adjusting the cable length," *IEEE/ASME Transactions on Mechatronics*, vol. 22, no. 5, pp. 2319–2329, Oct 2017.

[11] K. Yoshida, H. Kawabe, and K. Kawanishi, "Stabilizing control for a single pendulum by moving the center of gravity. an investigation by numerical experiment," in *Proceedings of 35th IEEE Conference on Decision and Control*, vol. 1, Dec 1996, pp. 1039–1040 vol.1.

[12] K. Yoshida, I. Kawanishi, and H. Kawabe, "Stabilizing control for a single pendulum by moving the center of gravity: theory and experiment," in *Proceedings of the 1997 American Control Conference (Cat. No.97CH36041)*, vol. 5, June 1997, pp. 3405–3410 vol.5.

[13] M. Anderle, W. Michiels, S. Čelikovský, and T. Vyhlídal, "Damping a pendulum's swing by string length adjustment - design and comparison of various control methods," in *Proceedings of the 2019 American Control Conference (ACC)*, July 2019, pp. 4399–4405.

[14] S. Čelikovský, M. Anderle, and T. Vyhlídal, "Underactuated pendulum damping by its length adjustment and passive output selection," in *Proceedings of the 2020 European Control Conference (ECC)*, July 2020, pp. 100–105.

[15] Milan Anderle, Pieter Appeltans, Sergej Čelikovský, Wim Michiels and Tomáš Vyhlídal, "Controlling the Variable Length Pendulum: Analysis and Lyapunov Based Design Methods," *Submitted*, 2021.

[16] S. Huang, W. Liang, and K. K. Tan, "Intelligent friction compensation: A review," *IEEE/ASME Transactions on Mechatronics*, vol. 24, no. 4, pp. 1763–1774, 2019.

[17] H. K. Khalil, *Nonlinear systems; 3rd ed.* Upper Saddle River, NJ: Prentice-Hall, 2002.